Isotopic Probes Yield Microscopic Constants: Separation of Binding Energy from Catalytic Efficiency in the Bovine Plasma Amine Oxidase Reaction†

Monica M. Palcic‡ and Judith Pollock Klinman*

ABSTRACT: Bovine plasma amine oxidase catalyzes the oxidative deamination of primary amines. The reaction can be viewed as two half-reactions: enzyme reduction by substrate followed by enzyme reoxidation by dioxygen. Anaerobic stopped-flow kinetic measurements of the first half-reaction indicate very large deuterium isotope effects for benzylamine, *m*-tyramine, and dopamine, $^{D}k = 13.5 \pm 1.3$, which are ascribed to an intrinsic isotope effect. From the insensitivity of these isotope effects to amine concentration, stopped-flow data provide substrate dissociation constants, K_1, and rate constants for the C–H bond cleavage step, k_3, directly. Steady-state isotope effects have also been measured for benzylamine and six ring-substituted phenethylamines. Whereas a small range of values for k_{cat}, 0.38–1.2 s^{-1}, and $^{D}k_{cat}$, 5.4–8.8, is observed, $k_{cat}/K_m = 1.3 \times 10^2$ to 3.8×10^4 M^{-1} s^{-1} and $^{D}(k_{cat}/K_m) = 5.6–16.1$ indicate a marked effect of ring substituent. As described earlier [Miller, S., & Klinman, J. P. (1982) *Methods Enzymol. 87*, 711], the availability of an intrinsic isotope effect for an enzymatic reaction permits calculation of microscopic constants from steady-state data. By employment of a minimal mechanism for bovine plasma amine oxidase involving a single precatalytic and multiple postcatalytic enzyme–substrate complexes, equations have been derived that allow calculation of k_3 and K_1 when $^{D}K_{eq} \simeq 1 < {}^{D}k$. Unexpectedly, in the case of K_1, we have shown that this parameter can be calculated from steady-state parameters without the requirement for an intrinsic isotope effect. This result should have general application to both ping-pong and sequential ternary-complex enzyme mechanisms. Of significance for future applications of steady-state isotope effects to the calculation of microscopic constants, values for K_1 and k_3 derived from steady-state parameters and single turnover measurements indicate excellent agreement. Compilation of parameters among six ring-substituted phenethylamines reveals alteration in ΔG for enzyme–substrate complex formation by 2.8 kcal/mol, together with an essentially invariant rate constant for C–H bond activation. A detailed discussion of the relevance of these findings to the interrelationship of binding energy and catalytic efficiency in enzyme reactions is presented.

Recent advances in the application of kinetic isotope effects to the study of enzyme reactions suggest that steady-state kinetic isotope effects can yield microscopic rate constants directly. This approach involves the comparison of observed isotope effects on V_{max} and V_{max}/K_m to an intrinsic isotope effect for the bond cleavage step [cf. Miller & Klinman (1982)]. The validity of calculated rate constants is dependent on the correct choice of a minimal kinetic mechanism for the enzyme reaction under investigation. Northrop has argued that interpretation of steady-state kinetic isotope effects on V_{max} requires a kinetic scheme in which three precatalytic enzyme substrate complexes have been introduced (Northrop, 1981). While computer simulations support a role for multiple precatalytic complexes in the expression of isotope effects on V_{max}, in general the magnitude of V_{max} isotope effects is significantly more sensitive to variation in rate constants for postcatalytic than precatalytic steps.

In the present study, we have carried out extensive investigations of deuterium isotope effects in the pre-steady-state and steady-state reactions catalyzed by bovine plasma amine oxidase. Previous investigations of plasma amine oxidase have shown that aldehyde and ammonia are produced anaerobically (Berg & Abeles, 1980). In addition, parallel line kinetics indicative of a ping-pong mechanism imply either an irreversible step or first product release prior to oxygen binding (Oi et al., 1970). A minimal mechanism consistent with these findings is

$$E_{ox} + RCH_2NH_3^+ \rightleftharpoons E_{ox}\cdot RCH_2NH_3^+ \xrightarrow[NH_3]{} E_{red}\cdot RCHO \quad (1)$$

$$E_{red}(RCHO) \xrightarrow{O_2,\ H_2O_2} E_{ox} + (RCHO) \quad (2)$$

According to (1) and (2), steady-state kinetics studies will reflect steps involving enzyme reduction by amine, eq 1, followed by enzyme reoxidation by dioxygen, eq 2. The aldehydic product is retained in eq 2, since it has not yet been established that aldehyde release is a prerequisite for enzyme reoxidation. In the case of anaerobic stopped-flow kinetic studies, direct isolation and characterization of the first half-reaction is possible. As demonstrated herein, the pre-steady-state oxidation of benzylamine, *m*-tyramine, and dopamine yields values for substrate dissociation constants and rate constants for enzyme reduction that are almost identical with those calculated from steady-state kinetic isotope effects on V_{max} and V_{max}/K_m. Thus, although multiple precatalytic complexes may exist in the plasma amine oxidase reaction, the available data support the use of a minimal kinetic scheme involving a single enzyme–substrate complex in the formulation of V_{max} isotope effects.

A consequence of these studies is the availability of binding and catalytic rate constants for the oxidation of benzylamines and a series of six ring-substituted phenethylamines. We report a large change in the free energy of formation of enzyme–substrate complex, together with an essentially invariant rate constant for C–H bond cleavage. This result was unexpected in the context of models that ascribe the catalytic efficiency

† From the Department of Chemistry, University of California, Berkeley, California 94720. *Received April 15, 1983; revised manuscript received July 15, 1983.* Supported by a grant from the National Science Foundation.

‡ Present address: Department of Chemistry, The Ohio State University, Columbus, OH 43210.

0006-2960/83/0422-5957$01.50/0

of enzyme reactions to a diversion of noncovalent binding interactions from tight enzyme–substrate complex formation to a reduction in the energy barrier between the E·S and E·S‡ complex [cf. Jencks (1975)]. The properties of bovine plasma oxidase that lead to this result are discussed and contrasted with enzymatic systems for which catalytic efficiency can only be achieved by the introduction of ground-state strain/transition-state stabilization.

Materials and Methods

All chemicals were obtained commercially and were reagent grade, unless otherwise indicated. (3-Methoxyphenyl)acetonitrile, (3,4-dimethoxyphenyl)acetonitrile, and $LiAl^2H_4$ (isotopic purity >98%) were obtained from Aldrich, benzonitrile and phenylacetonitrile were from Matheson Coleman and Bell, and $LiAlH_4$ was from Alfa Ventron. Bio-Rex AG 50W-X12 resin was from Bio-Rad Laboratories. Tetrahydrofuran was dried over Na/benzophenone and distilled immediately before use.

Enzymes. Liver alcohol dehydrogenase, glucose oxidase, and catalase were obtained from Sigma. Three forms of plasma amine oxidase, A_1, A_2, and B, were purified from beef blood as described by Summers et al. (1979). Activity was assayed spectrophotometrically with 10 mM benzylamine as substrate in 100 mM potassium phosphate buffer, pH 7.2, and monitoring the increase in absorbance at 250 nm due to benzaldehyde formation. The difference in molar extinction coefficients of benzylamine and benzaldehyde was taken as 12 800 (Neumann et al., 1975). The protein concentration was determined spectrophotometrically at 280 nm by using an $E^{1\%}_{1cm}$ of 20.8 (Yasunobu et al., 1976). The overall yield of purified plasma amine oxidase from 10 L of blood was 15%, and this consisted of 6, 14, and 7 units of specific activities of 0.24, 0.36, and 0.24 unit/mg for fractions A_1, A_2, and B, respectively.

Substrates. Phenethylamine hydrochloride, dopamine hydrochloride, and tyramine hydrochloride were supplied by Sigma. Benzylamine and 4-methoxyphenethylamine were obtained from Aldrich and converted to their hydrochloride salts by bubbling HCl(g) through ethereal solutions of the amines followed by recrystallization 2 times from methanol.

The syntheses of protonated and C-1 dideuterated phenethylamine, 4-methoxyphenethylamine, 3,4-dimethoxyphenethylamine, and 3-methoxyphenethylamine were carried out in parallel by the reduction of the corresponding nitrile and $LiAlH_4$, or $LiAl^2H_4$ and $AlCl_3$ under nitrogen in a modification of the method of Nystrom (1955). In a typical synthesis, 0.066 M of $AlCl_3$ in 100 mL of ether was added to 0.066 M $LiAlH_4$ or $LiAl^2H_4$ in 70 mL of ether. The suspension was stirred for 5 min, 0.066 M of the corresponding phenylacetonitrile was added dropwise over a 1-h period, and the reaction mixture stirred for an additional hour. Water (4 mL) was added cautiously to quench the reaction. The solution was acidified by the addition of 90 mL of 3 M H_2SO_4 and 70 mL of water, extracted with ether, and adjusted to pH 11 with the addition of solid KOH. The basic solution was extracted 4 times with 200 mL of ether, washed, and dried with sodium sulfate. HCl(g) was bubbled through the combined ethereal extracts forming the HCl salt. The precipitate was filtered and recrystallized from methanol.

m-Tyramine, *p*-tyramine, and dopamine were synthesized by the deprotection of 2 g of the appropriate methoxyphenethylamine hydrochloride by heating at reflux under N_2 for 6 h in 45 mL of 48% freshly distilled HBr. HBr was removed by evaporation under reduced pressure and exchanged 4 times with 4 M HCl, followed by recrystallization from methanol–ether. Dopamine and *m*-tyramine were further purified by passage over a Bio-Rex AG 50W-12 column equilibrated with 0.1 M HCl and eluted with 4 M HCl.

Benzylamine and [1,1-$^2H_2$]benzylamine were synthesized by following the procedure described by Bardsley et al. (1973), by the reduction of benzonitrile with $LiAl^2H_4$ or $LiAlH_4$ in anhydrous tetrahydrofuran.

^1H NMR (proton nuclear magnetic resonance) spectra of all dideuterated samples, determined on a Varian EM-390 spectrometer in D_2O, showed no detectable signal attributable to the methylene protons at C-1 of amine, indicating less than 5% contamination by nondeuterated material. The melting points of all synthesized substrates and mixtures of synthesized and authentic materials (when available) were identical.

Steady-State Kinetics. Initial velocity studies for both deuterated and protonated substrates were carried out at 25 °C in potassium phosphate buffer, pH 7.2, ionic strength 0.10. The rate of reactions was measured on a Cary 118 spectrophotometer by monitoring the increase in absorbance at 250 nm for benzaldehyde production or by monitoring O_2 consumption of air-saturated solutions on a Yellow Springs Instrument polarographic oxygen electrode. All data were fitted to eq 3 by using the FORTRAN program of Cleland (1979),

$$v = V_{max}S/(K_m + S) \quad (3)$$

which was translated to Basic for use on a Northstar Horizon computer. Enzyme activity has been normalized to an activity of 0.36 unit/mg, and first- and second-order rate constants have been calculated from V_{max} and V_{max}/K_m, respectively, by assuming a subunit molecular weight of 85 000. The three forms of plasma amine oxidase are kinetically indistinguishable when normalized to 0.36 unit/mg.

Mixing experiments utilizing 50:50 mixtures of protonated and deuterated substrates resulted in the predicted decrease in the magnitude of isotope effects, indicating the absence of enzyme inhibitors in deuterated samples. The K_m for oxygen with benzylamine as a substrate is very low, 1.4×10^{-5} M or 0.71% (Oi et al., 1970). A similar low K_m for O_2 is suggested for all substrates in this study, since identical initial rates were obtained when measured at 8–10% or 20% oxygen, indicating saturating oxygen concentrations under the conditions of these studies.

Pre-Steady-State Kinetics. Anaerobic stopped-flow measurements were carried out at 25 °C in potassium phosphate buffer, pH 7.2, ionic strength 0.10, on a modified Durum D-110 spectrophotometer interfaced with a Northstar Horizon II microcomputer provided by On-Line Instruments Systems. These modifications included replacement of drive syringes by gas-tight syringes. The valve blocks were also replaced with Luer-Lok fittings to allow samples to be transferred anaerobically.

Samples were made anaerobic by bubbling high-purity argon over gently stirred solutions of enzyme or substrate for 15 min (enzyme on ice). This was carried out in 25-mL round-bottom flasks sealed with a rubber septum. The enzyme solutions contained 1% poly(ethylene glycol) 6000 to prevent protein denaturation during bubbling. All solutions contained 50 mM glucose. After 15 min, glucose oxidase and catalase were added to the solutions at a final concentration of 0.4 μM and 42 mM, respectively, to scavenge any oxygen remaining. After 10 min, the solutions were transferred to the stopped-flow by syringe and left in the drive syringes 10–15 min to ensure temperature equilibration and allow depletion of any O_2 introduced by the transfer. The activity of the enzymes before bubbling with argon and after all measurements was unchanged within experimental error.

Table I: Stoichiometry of Enzyme Reduction in the Reductive Half-Reaction Catalyzed by Bovine Plasma Amine Oxidase

substrate	enzyme concn (μM)	enzyme sp act. (units/mg)	amplitude obsd[b]	amplitude calcd[c]
benzylamine	26	0.18	0.048	0.062
[1,1-$^2H_2$]-benzylamine	15	0.15	0.034	0.036
m-tyramine	8	0.14	0.018	0.019
dopamine	3	0.05	0.007	0.007

[a] Concentration of enzyme calculated from the number of milligrams in the reaction after mixing and the ratio of the observed specific activity to an optimal value of 0.36 unit/mg. [b] Change in absorbance at 480 nm. [c] Calculated from $A = \Delta\epsilon l[E]$ where $\Delta\epsilon = 1333\ M^{-1}\ cm^{-1}$ and $l = 1.8$ cm. These calculations assume two active sites per dimer of 170 000 daltons. It should be noted that although plasma amine oxidase loses activity with time, good agreement between calculated and observed amplitudes has been observed in all experiments.

The anaerobic reduction of plasma amine oxidase by excess amine substrates was monitored at 480 nm, which resulted in a decrease in absorbance as a function of time. A total of 250 data points were collected per experiment and stored on floppy diskettes. First-order rate constants were calculated and fitted to the experimentally recorded absorbance change by interactive analysis (Dyson & Isenberg, 1971). Four to six determinations of the rate constants were performed; these were averaged for a single value with known standard deviation. Following each measurement, solutions were collected, and the pH was measured.

Results

Stopped-Flow Kinetic Parameters. Stopped-flow kinetic experiments were carried out under conditions of substrate (0.04–24 mM) in excess over enzyme concentration (3–26 μM). Maintenance of anaerobic conditions has enabled us to monitor the stoichiometric formation of reduced, enzyme-bound cofactor (Table I). In all instances, this reduction was found to obey first-order kinetics, illustrated in Figure 1 for enzyme reduction by deuterated benzylamine. Previous stereochemical studies with dopamine suggested the presence of two catalytically competent binding modes for this substrate (Summers et al., 1979). The appearance of a single exponential process for enzyme reduction by dopamine implies either that both binding modes for dopamine turn over at comparable rates or that conformational equilibrium of dopamine at the enzyme active site is rapid relative to enzyme reduction.

Variation of amine concentration leads to saturation kinetics for all amines examined. Reciprocal plots of k_{obsd} vs. amine concentration are shown in Figure 2 for the oxidation of *m*-tyramine and [1,1-$^2H_2$]-*m*-tyramine. From the intercept

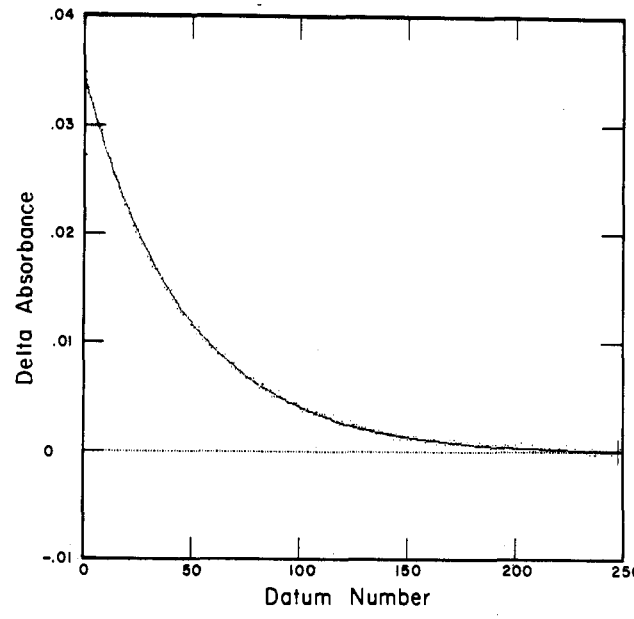

FIGURE 1: Stopped-flow trace of absorbance at 480 nm vs. time for anaerobic reduction of 15 μM plasma amine oxidase active sites by 7 mM [1,1-$^2H_2$]benzylamine. The collection time corresponds to 60 s. Experimental details of anaerobic stopped-flow kinetics are contained under Materials and Methods.

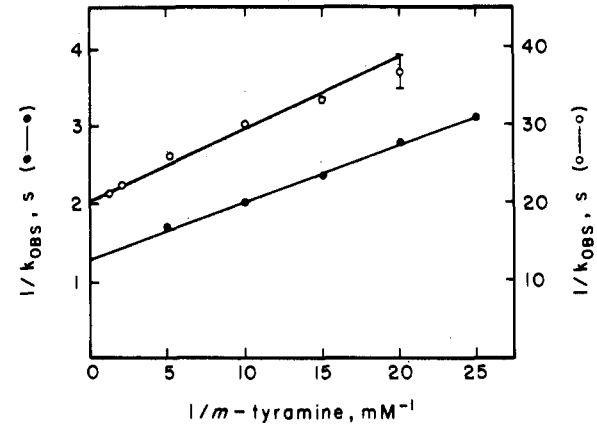

FIGURE 2: Reciprocal plots of observed rate constants, derived from anaerobic stopped-flow kinetic studies of plasma amine oxidase reduction by *m*-tyramine, as a function of *m*-tyramine (●) and [1,1-$^2H_2$]-*m*-tyramine (○).

values of the plots in Figure 2, it is apparent that substitution of deuterium for hydrogen at C-1 of substrate leads to a very large deuterium isotope effect. First- and second-rate constants were obtained from the intercepts and slopes of reciprocal plots according to Strickland et al. (1975):

$$E_{ox} + S \underset{k_2}{\overset{k_1}{\rightleftharpoons}} E_{ox}{\cdot}S \underset{k_4}{\overset{k_3}{\rightleftharpoons}} E_{red}{\cdot}P \qquad (4)$$

Table II: Anaerobic Stopped-Flow Kinetic Parameters and Deuterium Isotope Effects

substrate	k_3 (s^{-1})[a]	$^Dk_3$	k_3/K_1 ($M^{-1}\ s^{-1}$)	$^D(k_3/k_1)$
m-tyramine	0.763 ± 0.025	15.2 ± 0.7	$1.37 \pm 0.07 \times 10^4$	12.5 ± 1.4
dopamine	0.915 ± 0.033	12.1 ± 0.6	$1.99 \pm 0.08 \times 10^3$	13.3 ± 1.0
benzylamine	1.95 ± 0.05	15.0 ± 0.5	$4.55 \pm 0.16 \times 10^3$	12.6 ± 0.8
		av: 14.1 ± 1.7[b]		av: 12.8 ± 0.4[b]

[a] Kinetic parameters, which were obtained from the slopes and intercepts of reciprocal plots of k_{obsd} vs. amine concentration (Strickland et al., 1975), refer to Scheme I, where it is assumed that the extinction coefficient change for reduced enzyme is the same for enzyme-bound imine and enzyme-bound aldehyde plus ammonium ion. The actual rate constant for enzyme reduction will lie between k_3 and $k_3 + k_4$; from the observed stoichiometries for enzyme reduction, Table I, and linearity of reciprocal plots, Figure 2, we conclude that k_4 is small relative to k_3 or k_5. [b] Magnitude exceeds the semiclassical limit, and $^Dk = 13.5 \pm 1.3$ ascribed to an "intrinsic isotope effect" on the C-H bond cleavage step.

Table III: Kinetic Parameters and Deuterium Isotope Effects for Steady-State Oxidation of Aromatic Amines

substrate	k_{cat}/K_m (M^{-1} s^{-1})	$^D(k_{cat}/K_m)$	k_{cat} (s^{-1})	$^Dk_{cat}$
m-methoxyphenethylamine	$3.8 \pm 0.1 \times 10^4$	8.8 ± 0.5	1.2 ± 0.07	7.0 ± 1.0
m-tyramine	$4.3 \pm 0.5 \times 10^3$	8.6 ± 1.2	0.51 ± 0.03	6.5 ± 0.6
p-methoxyphenethylamine	$1.3 \pm 0.2 \times 10^3$	16.1 ± 1.3	0.40 ± 0.08	5.9 ± 1.2
dopamine	$1.2 \pm 0.07 \times 10^3$	6.5 ± 0.5	0.43 ± 0.01	5.6 ± 0.4
phenethylamine	$4.5 \pm 0.3 \times 10^2$	12.6 ± 1.1	0.38 ± 0.02	8.8 ± 0.5
benzylamine	$3.2 \pm 0.3 \times 10^2$	12.4 ± 1.0	0.54 ± 0.02	5.6 ± 0.3
p-tyramine[a]	$1.2 \pm 0.1 \times 10^2$	6.8 ± 1.1	0.15 ± 0.01	5.4 ± 0.4
	7.4 ± 0.8	5.6 ± 1.1	0.39 ± 0.04	5.7 ± 0.6

[a] Biphasicity observed in reciprocal plots. Upper entries derived from the low substrate concentration range.

As discussed by these authors, linearity of reciprocal plots implies that k_4 is small relative to k_3. Rate constants and isotope effects on these constants are summarized in Table II for enzyme reduction of *m*-tyramine, dopamine, and benzylamine. The data indicate similar, large primary isotope effects at both high and low substrate concentrations. Averaging of the isotope-effect data available from stopped-flow experiments provides a value of $^Dk = 13.5 \pm 1.3$.

It should be noted that isotope effects were obtained with amines dideuterated at C-1, leading to measured values that reflect the product of a primary and secondary effect. By employment of an upper limit for the secondary isotope effect correction of 1.4 (Klinman, 1978), a range for the primary deuterium isotope effect can be estimated to be $^Dk = 9.6$–13.5. These values are at (or exceed) the semiclassical limit for hydrogen-abstraction reactions (Bell, 1973), and we ascribe the observed isotope effects in the reductive half-reaction catalyzed by bovine plasma amine oxidase to the intrinsic isotope effect on the C–H bond cleavage step. The apparent insensitivity of ^Dk to substrate concentration, Table II, implies that substrate release from enzyme ternary complex is rapid relative to C–H bond abstraction; and hence, stopped-flow data provide the dissociation constants for amine release from enzyme (K_1) directly. A notable feature of the data in Table II is the invariance of the first-order rate constant to amine structure, together with a 30-fold change in K_1. This point will be addressed further, following presentation of steady-state data.

Steady-State Kinetic Parameters. Previous investigators have reported a remarkably broad substrate specificity for the bovine plasma amine oxidase oxidation of aliphatic and aromatic amines. In this study, we have focused on phenethylamines in an effort to determine the effect of remote ring substituent on catalytic parameters. In all cases, deuterium isotope effects have been measured in conjunction with initial rate parameters, providing k_{cat}, $^Dk_{cat}$, k_{cat}/K_m, and $^D(k_{cat}/K_m)$. As summarized in Table III, k_{cat} is largely unchanged for all substrates; from the diminished magnitudes of $^Dk_{cat}$ relative to $^Dk = 13.5$ observed under pre-steady-state conditions, we conclude that steps subsequent to enzyme reduction are partially rate limiting in the steady state. These steps may include either imine hydrolysis or enzyme reoxidation, eq 2 and 3 in Scheme I.

The second-order rate constant, k_{cat}/K_m, undergoes a 300–5000-fold increase in proceeding from the slowest, *p*-tyramine, to the fastest substrate, *m*-methoxyphenethylamine. Although *p*-tyramine was pure as accertained by NMR spectroscopy, it was important to establish that the very low observed rate with this substrate was not due to a trace (<5%) contaminant. Employing amine oxidase coupled to liver alcohol dehydrogenase, >9% of the *p*-tyramine was turned over as measured by the decrease in absorbance at 340 nm, confirming that k_{cat} and k_{cat}/K_m are those of *p*-tyramine and not an impurity. A second complicating feature regarding *p*-tyramine was an apparent biphasicity in double-reciprocal plots, which was independent of enzyme preparation or form (A_1, A_2, or B). We have reported data from both the low and high substrate concentration ranges, noting an approximately 2-fold change in k_{cat} together with an approximately 10-fold change in k_{cat}/K_m.

Scheme I: Minimal Mechanism for Reaction Catalyzed by Plasma Amine Oxidase That Includes Reductive Half-Reaction, Eq 1, Imine Hydrolysis, Eq 2, and Enzyme Reoxidation, Eq 3[a]

$$E_{ox} + RCH_2NH_3^+ \underset{k_2}{\overset{k_1}{\rightleftharpoons}} E_{ox} \cdot RCH_2NH_3^+ \underset{k_4}{\overset{k_3}{\rightleftharpoons}} E_{red} \cdot RCH{=}NH_2^+ \quad (1)$$

$$E_{red} \cdot RCH{=}NH_2^+ \xrightarrow{k_5} E_{red} \cdot RCHO \cdot NH_4^+ \quad (2)$$

$$E_{red}(RCHO \cdot NH_4^+) \xrightarrow[O_2 \quad H_2O_2]{k_6} E_{ox} + RCHO + NH_4^+ \quad (3)$$

[a] Equation 3 is a lumped expression containing oxygen binding and reduction. Since these studies were conducted under concentration of oxygen $> K_m$, k_6 can be attributed to the unimolecular rate constant for the conversion of $E_{red}(RCHO{\cdot}NH_4^+){\cdot}O_2$ to E_{ox} + RCHO + NH_4^+ + H_2O_2.

The isotope effects in k_{cat}/K_m are more variable than those on k_{cat}, ranging from 5.6 for *p*-tyramine to 16.1 for *p*-methoxyphenethylamine. The magnitude of $^D(k_{cat}/K_m)$ for the latter compound is larger than any other isotope effect observed in these studies, although within experimental error of $^Dk = 13.5 \pm 1.3$ derived from the stopped-flow experiments. Thus, we prefer to attribute this effect to error, while noting the possibility that the intrinsic isotope effect for *p*-methoxyphenethylamine may be anomalously high. In the case of phenethylamine and benzylamine, $^D(k_{cat}/K_m)$ is similar to ^Dk, and we conclude that k_{cat}/K_m is limited by the C–H bond abstraction step for *p*-methoxyphenethylamine, phenethylamine, and benzylamine. Diminution of $^D(k_{cat}/K_m)$ from ^Dk for the remaining amines could arise from either slow substrate release from the enzyme–substrate complex or possibly partial rate limitation from imine hydrolysis, which we ascribe to the first irreversible step, Scheme I.

In the case of dopamine and *m*-tyramine, stopped-flow data can distinguish these possibilities, since pre-steady-state isotope effects are expected to be insensitive to the rate of imine conversion to aldehyde and ammonia. As seen from Tables II and III, $^Dk = 13.5 \pm 1.3$ is ca. 2-fold larger than $^D(k_{cat}/K_m) = 6.5 \pm 0.5$ and 8.6 ± 1.3, implicating rapid release of dopamine and *m*-tyramine from the enzyme–substrate complex together with partial rate limitation by imine hydrolysis in the steady state. This result is not unexpected in the context of previous reports of a rapid exchange of tritium from [2-^{3}H]-dopamine in the course of its oxidation, attributed to the formation of an activated (imine) intermediate with a sufficient lifetime to permit full exchange from C-2:

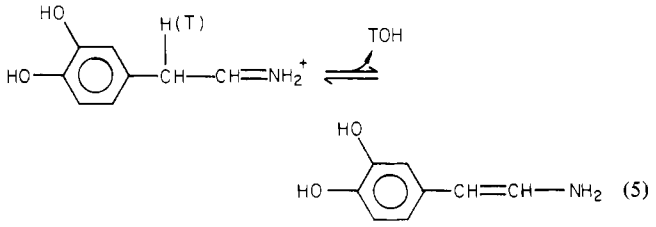

(5)

Although a single active site residue has been suggested to catalyze both substrate oxidation at C-1 and exchange at C-2, this proposal is inconsistent with the reduced magnitude of $^{D}(k_{cat}/K_m)$ for dopamine. If a single residue were catalyzing both oxidation and rapid exchange, irreversible loss of deuterium to solvent from [1-^{2}H]dopamine concomitant with its oxidation would cause the expression for $^{D}(k_{cat}/K_m)$ to be independent of all steps subsequent to substrate oxidation (Knowles & Albery, 1977). Thus, the observation that $^{D}(k_{cat}/K_m) < {}^{D}(k_3/K_1)$ suggests two bases at the active site of plasma amine oxidase, with the group catalyzing substrate oxidation at C-1 undergoing slow exchange and the group catalyzing proton abstraction from C-2 in rapid exchange with solvent.

Calculation of Microscopic Constants from Steady-State Data. Equations for initial rate parameters and isotope effects on these parameters are given in Table IV for the reaction mechanism in Scheme I. These equations incorporate a reversible step for the C–H bond abstraction step and, hence, contain $^{D}K_{eq}$, the equilibrium isotope effect for the conversion of E_{ox}–B·$RCH_2NH_3^+$ to E_{red}–BH·RCH=NH_2^+. As described previously, the availability of an intrinsic isotope effect on the bond cleavage step can provide microscope rate constants from steady-state parameters and isotope effects on these parameters (Miller & Klinman, 1982). In the case of plasma amine oxidase, the complexity of the minimal kinetic mechanism in Scheme I leads to four equations in seven unknowns. Thus, even with a value for the intrinsic isotope effect, exact solution for each microscopic rate constant is not possible.

A property of hydrogen-transfer reactions is the small magnitude of equilibrium isotope effects in relation to kinetic effects, with $^{D}K_{eq}$ expected to vary from 0.9 to 1.2 for a hydrogen transfer from carbon to an oxygen or nitrogen base (Klinman, 1978; Cleland, 1983). These low anticipated values for $^{D}K_{eq}$ relative to $^{D}k = 13.5$ in the plasma amine oxidase reaction indicate that the isotope-effect expression for k_{cat} and k_{cat}/K_m can be approximated by the form:

$$\text{I.E.(obsd)} = \frac{{}^{D}k + b}{1 + b} \qquad (6)$$

Under this condition, rearrangement of eq 1–4 in Table IV leads to exact solution for the rate constant for C–H bond cleavage, k_3, and substrate dissociation constant, K_1 (Table V).

Several unexpected features of steady-state isotope effects are evident from the equations in Table V: (i) *microscopic rate constants for chemical steps can be calculated for kinetically complex reactions characterized by more unknowns than equations* and (ii) *substrate dissociation constants are available from measured isotope effects on k_{cat} and k_{cat}/K_m, without the requirement for an intrinsic isotope effect.* Although eq 2 in Table V was derived for the first bound substrate of a ping-pong mechanism, it is a general equation and will pertain to the second bond substrate in a ternary-complex mechanism.

In Table VI, calculated values for k_3 and K_1 are compared to measured parameters for the three substrates studied in the pre steady state. Although values for k_3 derived from pre steady state may reflect the sum of the forward and reverse rate constants for enzyme reduction, the close correspondence between measured and calculated values for k_3 indicates that $k_4 < k_3$ and k_5 for the three substrates investigated. This result was implied from the observed linearity of reciprocal plots of k_{obsd} vs. amine concentration (Strickland et al., 1975) and from the observed stoichiometric reduction of enzyme by substrate in a single turnover for dopamine and *m*-tyramine (Table I), which in the context of partial rate limitation by imine hydrolysis in the steady state would have been less than unity had k_4 been comparable to k_3. Calculated values for K_1 are also in good agreement with measured values with the possible exception of that of *m*-tyramine. In light of our ability to calculate K_1 directly from experimentally measured isotope effects, the discrepancy between measured and calculated values for K_1 cannot be ascribed to misassignment of ^{D}k, and we are uncertain whether 56 or 160 μM better represents the correct dissociation constant for *m*-tyramine.

Similar calculations of k_3 and K_1 have been carried out from the available steady-state isotope effects for the remaining substrates in Table III. As seen in Table VII, the rate constant for C–H bond cleavage appears almost unaltered, k_3 = 0.61–2.5 s^{-1}, over a large change in binding energy. Thus, calculated values for k_3 and K_1 confirm the trend in rate and binding constants observed over a smaller series of substrates in pre-steady-state experiments.

Discussion

Calculation of Microscopic Rate Constants—What Constitutes a Minimal Mechanism? Although the potential for steady-state isotope effects to provide microscopic rate constants in enzyme reactions has been recognized (Miller & Klinman, 1982; Ahn & Klinman, 1983), the studies reported herein represent the first instance in which calculated constants have been compared to parameters derived from direct measurement. Thus, it is highly significant that measured and calculated constants are in close agreement. As demonstrated under Results, the method of calculation of k_3 and K_1 is a general one when $^{D}K_{eq} \simeq 1 < {}^{D}k$ and, hence, should be applicable to complex mechanisms involving multiple steps subsequent to the isotope-sensitive step.

Of particular note is our use of a single precatalytic enzyme–substrate complex in the formulation of a minimal mechanism. Northrop (1981) has discussed the role of precatalytic steps, arguing that three such steps constitute a minimal kinetic mechanism in the formulation of V_{max} isotope effects. Evidence presented in support of this conclusion is 2-fold: (i) the simulation of isotope effects under conditions where rate constants for the interconversion of precatalytic steps undergo large changes and (ii) the apparent demonstration that the magnitude of a deuterium isotope effect may be insensitive to a slow product release step if this step follows an irreversible step. Regarding the first point, it is clear that precatalytic steps may influence the magnitude of $^{D}V_{max}$. However, in general the magnitude of $^{D}V_{max}$ is considerably more sensitive to changes in the rate of postcatalytic than precatalytic steps; e.g., $^{D}V_{max}$ varied 270% for a 100-fold change in a postcatalytic step (Northrop, case 1), whereas similar changes in precatalytic rate constants led to only 25, 8, and 0% change in $^{D}V_{max}$ (Northrop, cases 2–4). Thus, our ability to neglect multiple, precatalytic steps in the calculation of rate constants for plasma amine oxidase does not necessarily imply that these steps are absent; alternatively, small changes in $^{D}V_{max}$ due to precatalytic steps may simply lie within the error bounds of measured and, hence, calculated parameters.

Table IV: Initial Rate Parameters and Deuterium Isotope Effects in Terms of Microsopic Rate Constants for the Kinetic Mechanism in Scheme I

parameter	isotope effect
$k_{cat} = \frac{k_3k_5k_6}{k_3k_5 + k_3k_6 + k_6(k_4 + k_5)}$ (1)	${}^{D}k_{cat} = \frac{{}^{D}k + k_{3H}/k_6 + k_{3H}/k_5 + {}^{D}K_{eq}k_{4H}/k_5}{1 + k_{3H}/k_6 + k_{3H}/k_5 + k_{4H}/k_5}$ (3)
$k_{cat}/K_m = \frac{k_1k_3k_5}{k_2(k_4 + k_5) + k_3k_5}$ (2)	${}^{D}(k_{cat}/K_m) = \frac{{}^{D}k + k_{3H}/k_2 + {}^{D}K_{eq}k_{4H}/k_5}{1 + k_{3H}/k_2 + k_{4H}/k_5}$ (4)

Table V: Expressions and Error Function for k_3 and K_1 in Terms of Steady-State Parameters and Isotope Effects on These Parameters and the Intrinsic Isotope Effect[a]

constant	error function
$k_3 = \frac{k_{cat}({}^{D}k - 1)}{{}^{D}k_{cat} - 1}$ (1)	$\frac{\sigma k_3}{k_3} = \left(\left(\frac{\sigma {}^{D}k}{{}^{D}k - 1}\right)^2 + \left[\frac{\sigma k_{catH}}{k_{catH}({}^{D}k_{cat} - 1)}\right]^2 + \left[\frac{\sigma k_{catD}\,{}^{D}k_{cat}}{k_{catD}({}^{D}k_{cat} - 1)}\right]^2\right)^{1/2}$ (3)
$K_1 = \frac{k_{cat}[{}^{D}(k_{cat}/K_m) - 1]}{(k_{cat}/k_m)({}^{D}k_{cat} - 1)}$ (2)	$\frac{\sigma K_1}{K_1} = \left(\left(\frac{\sigma k_{catH}}{k_{catH}({}^{D}k_{cat} - 1)}\right)^2 + \left[\frac{\sigma k_{catD}\,{}^{D}k_{cat}}{k_{catD}({}^{D}k_{cat} - 1)}\right]^2 + \left[\frac{(\sigma k_{cat}/K_m)_H}{(k_{cat}/K_m)_H({}^{D}k_{cat}/K_m - 1)}\right]^2 + \left[\frac{(\sigma k_{cat}/K_m)_D\,{}^{D}(k_{cat}/K_m)}{(k_{cat}/K_m)_D[{}^{D}(k_{cat}/K_m) - 1]}\right]^2\right)^{1/2}$ (4)

[a] The error functions, eq 3 and 4, were derived as described in Miller & Klinman (1982).

Table VI: Comparison of Calculated to Measured Constants

substrate	k_3 (s^{-1})		K_1 (mM)	
	SF[a]	SS[b]	SF[a]	SS[b]
m-tyramine	0.76 ± 0.03	1.2 ± 0.16	0.056 ± 0.006	0.16 ± 0.02
dopamine	0.92 ± 0.03	1.2 ± 0.17	0.46 ± 0.02	0.43 ± 0.05
benzylamine	2.0 ± 0.05	1.5 ± 0.16	4.3 ± 0.2	4.2 ± 0.1

[a] Stopped flow, direct measurement. [b] Steady state, calculated from eq 1 and 2, Table V.

Table VII: Calculated Microscopic Constants for Oxidative Deamination of Aromatic Amines

substrate	k_3 (s^{-1})	K_1 (M)	$-\Delta G$ (kcal/mol)
m-methoxyphenethylamine	2.5 ± 0.4	$4.1 \pm 0.6 \times 10^{-5}$	6.0
m-tyramine	1.2 ± 0.2	$1.6 \pm 0.2 \times 10^{-4}$	5.2
p-methoxyphenethylamine	1.0 ± 0.1	$9.5 \pm 0.7 \times 10^{-4}$	4.1
dopamine	1.2 ± 0.2	$4.3 \pm 0.5 \times 10^{-4}$	4.6
phenethylamine	0.61 ± 0.07	$1.2 \pm 0.1 \times 10^{-3}$	3.9
benzylamine	1.5 ± 0.2	$4.2 \pm 0.1 \times 10^{-3}$	3.2
p-tyramine[a]	0.85 ± 0.11	$1.7 \pm 0.3 \times 10^{-3}$	3.8
	1.0 ± 0.1	$5.2 \pm 1.1 \times 10^{-2}$	1.8

[a] Biphasicity observed in reciprocal plots. Upper entries derived from the low substrate concentration range. On the assumption that rates in this concentration range reflect only one of two sites per dimer, k_3 has been corrected to correspond to turnover of all subunits.

A second, potentially more compelling, point raised by Northrop concerns the independence of ${}^{D}V_{max}$ to events following the first irreversible step. The mechanism discussed by Northrop is

$$E_1 + S \underset{k_2}{\overset{k_1}{\rightleftharpoons}} E_2 \underset{k_4}{\overset{k_3}{\rightleftharpoons}} E_3 \underset{k_6}{\overset{k_5}{\rightleftharpoons}} E_4 \underset{k_8^*}{\overset{k_7^*}{\rightleftharpoons}} E_5 \underset{k_{10}}{\overset{k_9}{\rightleftharpoons}} E_6 \xrightarrow{k_{11}} E_7 \xrightarrow{k_{13}} E_8 \quad (7)$$

where k_7^* is the isotope-sensitive step and k_{11} is the first of two irreversible steps, e.g., the loss of first product in an enzymatic reaction generating two products. The expression defined by Northrop for ${}^{D}V_{max}$ corresponding to eq 7 is

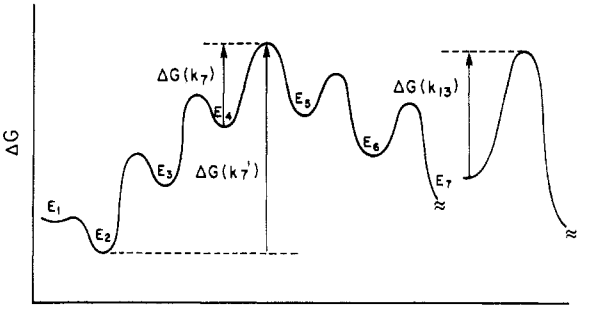

FIGURE 3: Free-energy profile for enzyme mechanism of eq 7 in the text, where $k_4 \gg k_3$, $k_6 \gg k_5$, and $[S] \gg K_m$.

$$ {}^{D}V_{max} = \frac{\frac{k_{7H}}{k_{7D}} + \frac{R_f}{E_f} + {}^{D}K_{eq}C_r}{1 + \frac{R_f}{E_f} + C_r} \quad (8)$$

where

$$R_f = \frac{k_{7H}}{k_5}\left(1 + \frac{k_4 + k_5}{k_3}\right) + \frac{k_{7H}}{k_{11}}\left(1 + \frac{k_{10} + k_{11}}{k_9}\right) + \frac{k_{7H}}{k_{13}}$$

$$E_f = 1 + \frac{k_6}{k_5}\left(1 + \frac{k_4}{k_3}\right)$$

$$C_r = \frac{k_8}{k_9}\left(1 + \frac{k_{10}}{k_{11}}\right)$$

In the case of an uphill process for the interconversion of $E_2 \rightleftharpoons E_3$, $k_4 \gg k_3$, and $E_3 \rightleftharpoons E_4$, $k_6 \gg k_5$, Figure 3 (Northrop's expanded case 5c), E_f will be approximated by the product of k_4/k_3 and k_6/k_5. Under this circumstance of $E_f = (k_4/k_3)(k_6/k_5) \gg 1$, R_f/E_f is expected to be small and to make a negligible contribution to the magnitude of ${}^DV_{max}$. According to the formalism of eq 8, the rate constant for the second of two irreversible steps (k_{13}) appears solely in R_f/E_f; i.e., it is not contained in the postcatalytic partitioning ratio and, hence, is expected to have a minimal impact on ${}^DV_{max}$ when $E_f \gg 1$. This property of eq 8 led Northrop to conclude that the observed isotope effect on V_{max} could remain large, approaching the intrinsic value, even in the event of a slow product release step subsequent to a first irreversible step.

The above conclusion, which appears to contradict intuition, is a consequence of the separation of kinetic functions, R_f, from equilibrium functions, E_f, in Northrop's definition of ${}^DV_{max}$. A common reaction mechanism encountered in physical–organic chemistry is one that proceeds via multiple reversible processes prior to the rate-determining step:

$$S_1 \overset{K_1}{\rightleftharpoons} S_2 \overset{K_2}{\rightleftharpoons} S_3 \overset{k}{\longrightarrow} P \qquad (9)$$

By definition for eq 9, k is the rate-determining step, that is, the process that crosses the highest point on the free-energy profile, Figure 4. However, the rate constant for the appearance of product is $k' = K_1K_2k$, and the relevant barrier height describing this process is the difference in energy between S_1 and S^*, $\Delta G(k')$ in Figure 4. Analogous treatment of the enzyme mechanism illustrated in Figure 3 dictates a redefinition of $k'_{7H} = (k_3/k_4)(k_5/k_6)k_{7H}$ with the resulting expression for ${}^DV_{max}$:

$${}^DV_{max} = \frac{k_{7H}/k_{7D} + b + {}^DK_{eq}C_r}{1 + b + C_r} \qquad (10)$$

$$b = \frac{k'_{7H}}{k_5}\left(1 + \frac{k_4 + k_5}{k_3}\right) + \frac{k'_{7H}}{k_{11}}\left(1 + \frac{k_{10} + k_{11}}{k_9}\right) + \frac{k'_{7H}}{k_{13}}$$

and

$$C_r = \frac{k_8}{k_9}\left(1 + \frac{k_{10}}{k_{11}}\right)$$

According to eq 10, terms influencing the expression of the intrinsic isotope effect contain the partitioning ratios k'_{7H}/k_5, k'_{7H}/k_{11}, k'_{7H}/k_{13}, and k_{8H}/k_9. This treatment correctly predicts a similar form for the sensitivity of the observed isotope effect to the postcatalytic rate constants, k_{11} and k_{13}, and we conclude that *the expression of k_{7H}/k_{7D} is not insensitive to the second of two irreversible steps when the barrier height controlling the isotope-sensitive step is correctly defined for comparison to the barrier heights of postcatalytic steps.*

It is of value to consider the form of eq 1 and 2, Table V, for kinetic mechanisms involving multiple precatalytic enzyme–substrate complexes. Combination of k_{cat} and ${}^Dk_{cat}$ for the kinetic mechanism in eq 7 leads to the following equation for the isotope-sensitive step (k_7):

$$\frac{k_7}{1 + k_6/k_5(1 + k_4/k_3)} = \frac{k_{cat}({}^Dk - 1)}{{}^Dk_{cat} - 1} \qquad (11)$$

In the event of energetically favorable interconversions for $E_2 \rightleftharpoons E_3$ and $E_3 \rightleftharpoons E_4$, k_6/k_5 and $k_4/k_3 \ll 1$, k_7 is obtained directly from k_{cat}, ${}^Dk_{cat}$, and ${}^Dk$. Alternatively, in the case of

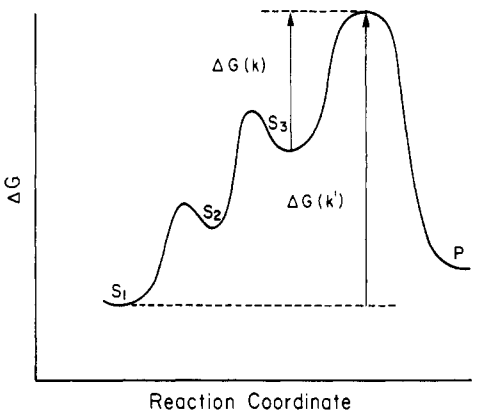

FIGURE 4: Free-energy profile for reaction mechanism of eq 9 in the text.

energetically unfavorable precatalytic interconversion steps, k_6/k_5 and $k_4/k_3 \gg 1$ (e.g., Figure 3), the correct rate constant reflecting the difference in energy between the stable ES and ES* complexes, $k'_7 = (k_3/k_4)(k_5/k_6)k_7$, would be calculated as long as k_4 and $k_6 > k_7$. Only in the latter situation where k_4 or $k_6 < k_7$, or in the case of a significant population of all precatalytic enzyme–substrate complexes, $k_6 \simeq k_5$ and $k_4 \simeq k_3$, would the rate constants calculated from eq 11 be incorrect. In this instance, calculated constants are expected to be reduced relative to k_7 and different from pre-steady-state parameters.[1] With the exception of K_1 for *m*-tyramine, comparison of calculated and observed constants for the plasma amine oxidase reaction, Table VI, indicates good agreement; and we conclude that Scheme I adequately describes the plasma amine oxidase reaction.

As the above discussion indicates, theoretical considerations support a relatively minor impact of multiple precatalytic ES complexes on the expression of V_{max} isotope effects. Experimental support for the use of minimal mechanisms involving a single ES complex derives from the data presented in this paper for the reaction catalyzed by plasma amine oxidase. Whereas further experimentation in other enzyme systems is required before completely general statements can be made, the arguments and data presented herein imply that the formulation of steady-state isotope effects can be made in the context of a single ES complex, permitting calculation of microscopic constants from initial rate parameters and intrinsic, V_{max} and V_{max}/K_m isotope effects.

Relationship of Binding Energy to Catalytic Efficiency. A role for substrate binding interactions in the generation of both specificity and catalytic efficiency in enzyme reactions is generally acknowledged. A major hypothesis, formulated by Jencks (1975), invokes utilization of intrinsic enzyme–substrate binding interactions to reduce the barrier between the ES and ES* complexes, expressed either as ground-state strain or transition-state stabilization. A significant number of experimental systems for which it has been possible to determine K_m and k_{cat} as a function of substrate structure support a utilization of substrate binding energy to increase k_{cat} (Ray & Long, 1976; Thompson, 1974; Sachdev & Fruton, 1970; Moore & Jencks, 1982). Thus, the possibility existed in the plasma amine oxidase reaction that changes in substrate structure remote from the carbon center undergoing oxidation would result in relatively unchanged binding parameters, to-

[1] Consider, for example, a kinetic situation in which k_3/k_4 and $k_5/k_6 = 1$ and k_7 is clearly rate determining. From pre-steady-state kinetics, $k_{obsd} = (k_3/k_4)(k_5/k_6)k_7 = k_7$, and from steady-state kinetics, $k_{calcd} = k_7/1 + k_6/k_7(1 + k_4/k_3) = 0.33k_7$.

Table VIII: Comparison of Calculated to Observed Free Energies of Binding for Ring-Substituted Phenethylamines

substrate	phenethylamine skeleton	substituent[a]		ΔG (kcal/mol)	
		hydrophobic[b]	H bond[c]	calcd	obsd
m-CH_3O-C_6H_4-$CH_2CH_2NH_3^+$	−3.9	+0.06	−2.5	−6.3	−6.0
m-HO-C_6H_4-$CH_2CH_2NH_3^+$	−3.9	+0.90	−2.5	−5.5	−5.2
H_5C_6-$CH_2CH_2NH_3^+$	−3.9				−3.9
p-CH_3O-C_6H_4-$CH_2CH_2NH_3^+$	−3.9	+0.06		−3.8	−4.1
p-HO-C_6H_4-$CH_2CH_2NH_3^+$	−3.9	+0.9		−3.0	−3.8
3,4-$(HO)_2$-C_6H_3-$CH_2CH_2NH_3^+$	−3.9	+1.8	−2.5	−4.6	−4.6

[a] Relative to phenethylamine. [b] The decrease in substrate affinity due to replacement of hydrogen by the more hydrophilic substituents, methoxy and hydroxyl. See text for further details. [c] The increase in substrate affinity due to replacement of hydrogen by meta substituents capable of serving as a hydrogen-bond acceptor. See text for further details.

gether with an enhancement of the (partially) rate-limiting C–H bond cleavage step.

The availability of K_1 and k_3 in the plasma amine oxidase reaction, Table VII, allows us to compare microscopic constants as opposed to K_m and k_{cat}. The overall change in the free energy of binding for the series of phenethylamines investigated is dependent on the value of K_1 chosen for *p*-tyramine. As noted under Results, reciprocal plots of steady-state data are biphasic for this substrate. Although data at low substrate concentration are difficult to obtain due to slow observed rates, the biphasicity is reproducible and unique to *p*-tyramine. As seen from Table III, k_{cat} values obtained from the low vs. high substrate concentration ranges for *p*-tyramine differ ca. 2-fold, suggestive of negative cooperativity in the binding of *p*-tyramine to the second of two subunits in the plasma amine oxidase dimer. Thus, the very large value of K_1 derived from the high substrate range may reflect site–site interactions. By employment of the K_1 derived from the low substrate range as a more conservative estimate of *p*-tyramine binding interactions, the overall change in the free energy of binding of ring-substituted phenethylamines to plasma amine oxidase is concluded to be 2.8 kcal/mol. Concomitant with this large change in binding energy, we fail to see a significant change in either the rate constant for the C–H bond cleavage step (Table VII) or k_{cat} (Table III).

The finding that binding energy and the rate constant for C–H bond cleavage are uncorrelated in the plasma amine oxidase reaction was unexpected. Clearly, some of the intrinsic binding energy of amines has been used to overcome the entropy barrier in this reaction, via anchoring of substrate in close proximity to active site catalytic residues. However, structural alterations in substrates fail to produce further increases in k_3 or k_{cat}, despite the fact that the reaction catalyzed by plasma amine oxidase is very slow. The broad substrate specificity exhibited by this enzyme has been noted (Yasunobu et al., 1976) and could, in principal, preclude the requisite specific interactions between substrate and enzyme that allow conversion of binding energy to a reduction in k_{cat}. In an effort to address this possibility, we have analyzed the effect of ring substituent on phenethylamine binding, Table VIII. The values for ΔG(obsd) in Table VIII indicate two important trends: (1) the methoxy substituent is better bound than the hydroxyl substituent, independent of whether substituents are in the meta or para positions, and (ii) placement of either substituent in the meta as opposed to para position leads to tighter binding. The difference between methoxy and hydroxyl binding is quantitatively similar to the difference in the free energy of partitioning of an aromatic methoxy vs. hydroxyl group between 1-octanol and water, estimated as 0.8 kcal/mol. This apolar preference is an indication of a hydrophobic active site, and we assign values of 0.06 and 0.90 kcal/mol for the decrease in substrate affinity following substitution of hydrogen by methoxy and hydroxyl, respectively (Leo et al., 1971; Fersht, 1977).

The effect of substituent position on the binding of phenethylamines suggests a further protein-mediated effect, which enhances the affinity of meta-substituted substrates. Since the hydroxyl and methoxy groups can both serve as hydrogen-bond acceptors (whereas only the hydroxyl group can behave as a hydrogen-bond donor), hydrogen bonding from a protein side chain to the meta substituent would explain the preferential binding of meta-substituted phenethylamines. The energetics of intramolecular hydrogen-bond formation are difficult to quantitate. Model studies have shown the enthalpy of hydrogen-bond formation between amides to be highly solvent dependent; e.g., $\Delta H = 0.0$ in water vs. −4.2 kcal/mol in carbon tetrachloride, Klotz & Franzen (1962). Energetics of hydrogen-bond formation have also been determined from heats of sublimation of crystallized amides, with values in the range of −5 kcal/mol, Hagler et al. (1974). From such studies we estimate −2.5 kcal/mol to be a reasonable value for the increase in binding energy resulting from hydrogen-bond formation within a preformed complex in a hydrophobic pocket. As indicated in Table VIII, employing this value for meta-specific hydrogen bonding, together with the changes in free energy anticipated from hydrophobic interactions, we obtain close agreement between calculated and observed free energies of binding. Whereas further studies with a wider range of substituents are necessary to both confirm this model and examine the role of steric effects on binding, the data in Table VIII implicate specific protein–substrate interactions at the plasma amine oxidase active site.

Possible insight into the role of these binding interactions in plasma amine oxidase catalysis may derive from considerations of the magnitude of enzymatic K_m values relative to physiologic substrate concentrations. Atkinson (1969) has argued that optimal efficiency and control of fluxes of metabolic intermediates will result when physiologic substrate concentrations are in the range of K_m. Similarly, in the context of models for the optimization of enzymatic activity, Fersht (1974) and Cornish-Bowden (1975) have concluded that K_m will approximate the concentration of substrate in vivo. Despite the difficulties in assessing intracellular metabolic pools, experimental support for $0.1 < [S]/K_m < 1$ is provided by data for the majority of glycolytic enzymes (Lowry & Passoneau, 1964).

Two extreme mechanisms for the evolution of enzymes characterized by K_m values approximating physiologic substrate concentrations can be envisaged. One mechanism [cf. Fersht (1974, 1977)] views an enzyme precursor as a protein capable of tight binding to substrate, Figure 5A. Achievement of enhanced catalytic efficiency is then achieved through a destabilization of the enzyme–substrate complex, leading to a reduced barrier for k_{cat} and increased values for K_m. Al-

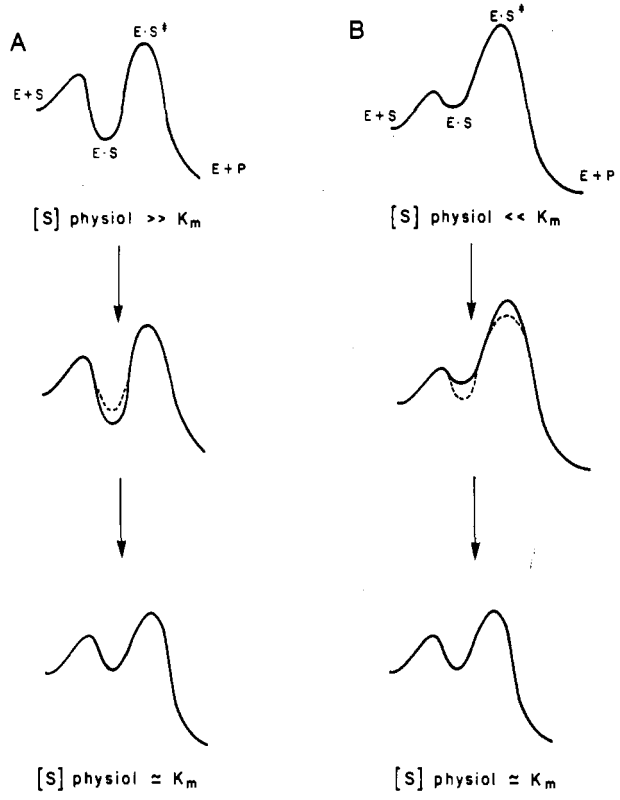

FIGURE 5: Mechanisms for evolution of enzymes for which the value of K_m approximates physiological substrate concentration, [S]: (A) evolution away from tight binding; (B) evolution toward tight binding.

ternatively, enzymes can be viewed as proteins that are evolving from weak to tight binding of substrate, Figure 5B. In this model, substrate concentrations are initially below K_m, such that k_{cat}/K_m is the relevant rate parameter. Enhancement of enzyme–substrate binding interactions can then be expressed equally well in both the enzyme–substrate and enzyme–transition-state complexes, allowing k_{cat}/K_m to rise and K_m to approach [S]. An advantage of the model in Figure 5B is that increased catalytic efficiency can be achieved without the introduction of ground-state destabilization until $K_m \simeq$ [S].

The very broad substrate specificity of plasma amine oxidase suggests a physiologic role for this enzyme in the deamination of a wide range of biogenic primary amines. The concentration of each amine in plasma is likely to be low relative to the K_m values measured in this study; e.g., the plasma concentration of dopamine is estimated as ≤4 nM (Wang et al., 1975) vs. a K_m = 360 μM (from the data in Table III), with the consequence that plasma amine oxidase will function under k_{cat}/K_m conditions. In this circumstance, the model in Figure 5B provides a mechanism for the utilization of substrate binding energy in the plasma amine oxidase via a simultaneous decrease in the energy levels of both enzyme–substrate and enzyme–transition-state complexes relative to free enzyme and substrate, leading to enhanced catalytic efficiency as long as [S] remains below K_m.

Analogous to plasma amine oxidase, numerous enzymes are known to be characterized by low turnover numbers and broad substrate specificities, e.g., glutathione transferase (Jacoby, 1978) and cytochrome P-450 (White & Coon, 1980). For such enzyme systems, the concentration of each substrate within a large pool of homologous substrates is likely to be low. Hence, remote binding interactions may lead to decreases in K_m, increases in k_{cat}/K_m, and unchanged k_{cat} values as we observe for plasma amine oxidase. Examination of initial rate parameters for the isozymes of glutathione transferase with a wide range of substrates provides some support for this concept. Whereas changes in k_{cat} occur as a function of substrate structure, these changes can be attributed in part to differences in chemical reactivity. Significantly, for each isozyme of glutathione investigated, observed increases in k_{cat}/K_m exceed those in k_{cat} by 1–2 orders of magnitude (Jacoby, 1978).

It is important to note that for enzymes in which catalytic efficiency and specificity arise from decreases in K_m, a "crossover" point must arise when K_m is reduced to the magnitude of [S]. At this juncture, it is no longer possible to increase rate in a simple manner via tighter binding of substrate, introducing the requirement for a selective use of binding energy to stabilize the transition state. The value of k_{cat}/K_m that characterizes this crossover point is likely to be a complex function of the inherent reactivity of the bond undergoing cleavage as well as the lower limit of substrate concentration that will permit effective turnover. Regarding k_{cat}, it may be that increases in this parameter beyond low values, e.g., $k_{cat} \simeq 1\ s^{-1}$ in the plasma amine oxidase reaction, do not become significant until K_m has been reduced to the level of [S].

Recently, Hall (1981) has investigated the directed evolution of a *lac* Z deletion strain of *Escherichia coli*, selecting for mutants that are capable of growth on lactose and other disaccharides via the production of altered forms of a second β-galactosidase gene product (initially specific for *o*-nitrophenyl and *p*-nitrophenyl β-galactosides). Kinetic analysis of these altered enzymes relative to wild-type enzyme reveals much faster decreases in K_m than increases in k_{cat}. In addition, k_{cat}/K_m is observed to increase for *all* substrates, while k_{cat} has been diminished 100-fold for *o*-nitrophenyl β-galactoside to a similar low value of ca. 1–2 s^{-1} for all substrates. A possible mechanism for the observed enhancements in k_{cat}/K_m is the evolution of enzymes that are capable of increased binding interactions between the galactosyl ring of both mono- and disaccharides, leading to a reduction in the energy barrier for the formation of galactosyl enzyme from free enzyme and substrate. Stabilization of the galactosyl enzyme intermediate would also provide a rationale for the reduction in k_{cat} observed for the preferred substrates of the wild-type enzyme, *o*-nitrophenyl and *p*-nitrophenyl β-galactoside. It will be of interest to see if continued selection for mutants that display a high degree of specificity toward a single disaccharide substrate results in relatively small changes in K_m, together with a large increase in the rate of hydrolysis of galactosyl enzyme.

Further investigations of the role of binding interactions in a wide range of enzyme systems may lead to generalizations regarding the magnitude of k_{cat}, the breadth of substrate specificity, and the mechanism whereby binding energy is utilized in catalysis. It should be emphasized that the above discussion has focused on enzyme systems for which [S] ≤ K_m. In the case of extracellular proteases, these enzymes are characterized by K_m values much lower than their physiological substrate concentrations [cf. Cornish-Bowden (1975)]. For enzymes of this class, the only mechanism available for an increase in rate is via a reduction in the barrier between the enzyme–substrate and enzyme–transition-state complexes. Thus, it is not surprising that investigations of the effect of substrate structure on kinetic parameters for elastase (Thompson, 1974), chymotrypsin (Baumann et al., 1973), and pepsin (Sachdev & Fruton, 1970) indicate essentially constant values for K_m, together with large variations in the magnitude of k_{cat}.

Acknowledgments

We thank Julie Bertucelli for technical assistance in steady-state kinetic studies of *p*-tyramine and Dr. Mazhar Husain for advice regarding the maintenance of anaerobic conditions for stopped-flow kinetic studies.

Registry No. Amine oxidase, 9059-11-4; *m*-tyramine, 588-05-6; dopamine, 51-61-6; benzylamine, 100-46-9; *m*-methoxyphenethylamine, 55-81-2; *p*-methoxyphenethylamine, 55-81-2; phenethylamine, 64-04-0; *p*-tyramine, 51-67-2.

References

Ahn, N., & Klinman, J. P. (1983) *Biochemistry 22*, 3096.
Atkinson, D. (1969) *Curr. Top. Cell. Regul. 1*, 29.
Bardsley, W. G., Crabbe, M. J. C., & Shindler, J. S. (1973) *Biochem. J. 131*, 459.
Baumann, W. K., Bizzozero, S. A., & Dutler, H. (1973) *Eur. J. Biochem. 39*, 381.
Bell, R. P. (1973) *The Proton in Chemistry*, Chapter 12, Cornell University Press, Ithaca, NY.
Berg, K. A., & Abeles, R. H. (1980) *Biochemistry 19*, 3186.
Cleland, W. W. (1979) *Methods Enzymol. 63*, 103.
Cleland, W. W. (1983) *CRC Crit. Rev. Biochem. 13*, 385.
Cornish-Bowden, A. (1975) *J. Mol. Biol. 101*, 1.
Dyson, R. D., & Isenberg, I. (1971) *Biochemistry 10*, 3233.
Fersht, A. R. (1974) *Proc. R. Soc. London, Ser. B 187*, 397.
Fersht, A. R. (1977) *Enzyme Structure and Mechanism*, Chapter 9, W. H. Freeman, Reading, PA, and San Francisco, CA.
Hagler, A. T., Lifson, S., & Huler, E. (1974) in *Peptides, Polypeptides and Proteins* (Blaut, E. R., Bovey, F. A., Goodman, M., & Lotan, N., Eds.) Wiley, New York.
Hall, B. G. (1981) *Biochemistry 20*, 4042.
Jacoby, W. B. (1978) *Adv. Enzymol. Relat. Areas Mol. Biol. 46*, 383.
Jencks, W. P. (1975) *Adv. Enzymol. Relat. Areas Mol. Biol. 43*, 219.
Klinman, J. P. (1978) *Adv. Enzymol. Relat. Areas Mol. Biol. 46*, 415.
Klotz, I. M., & Franzen, J. S. (1962) *J. Am. Chem. Soc. 84*, 3461.
Knowles, J. R., & Albery, W. J. (1977) *Acc. Chem. Res. 10*, 105.
Leo, A., Hansch, C., & Elkins, C. (1971) *Chem. Rev. 71*, 525.
Lowry, O. H., & Passoneau, J. V. (1964) *J. Biol. Chem. 239*, 31.
Miller, S., & Klinman, J. P. (1982) *Methods Enzymol. 87*, 711.
Moore, S. A., & Jencks, W. P. (1982) *J. Biol. Chem. 257*, 10893.
Neumann, R., Hevey, R., & Abeles, R. H. (1975) *J. Biol. Chem. 250*, 6362.
Northrop, D. B. (1981) *Biochemistry 20*, 4056.
Nystrom, R. F. (1955) *J. Am. Chem. Soc. 77*, 2544.
Oi, S., Inamasu, M., & Yasunobu, K. T. (1970) *Biochemistry 9*, 3370.
Ray, W. J., Jr., & Long, J. W. (1976) *Biochemistry 15*, 3993.
Sachdev, G. P., & Fruton, J. S. (1970) *Biochemistry 9*, 4465.
Strickland, S., Palmer, G., & Massey, V. (1975) *J. Biol. Chem. 250*, 4048.
Summers, M. C., Markovic, R., & Klinman, J. P. (1979) *Biochemistry 18*, 1969.
Thompson, R. C. (1974) *Biochemistry 13*, 5495.
Wang, M.-T., Imai, K., Yoshioka, M., & Tamura, Z. (1975) *Clin. Chim. Acta 63*, 13.
White, R. E., & Coon, M. J. (1980) *Annu. Rev. Biochem. 49*, 315.
Yasunobu, K. T., Ishitaki, H., & Minamiura, N. (1976) *Mol. Cell. Biochem. 13*, 3.